the FEBS Journal

# The A domain of fibronectin-binding protein B of *Staphylococcus aureus* contains a novel fibronectin binding site

Fiona M. Burke[1], Antonella Di Poto[2], Pietro Speziale[2] and Timothy J. Foster[1]

1 Department of Microbiology, Moyne Institute of Preventive Medicine, University of Dublin, Trinity College, Dublin, Ireland
2 Department of Biochemistry, University of Pavia, Pavia, Italy

**Keywords**
adhesion; fibrinogen; fibronectin; *Staphylococcus*; surface protein

**Correspondence**
T. J. Foster, Department of Microbiology, Moyne Institute of Preventive Medicine, University of Dublin, Trinity College, Dublin, Ireland
Fax: 0035316799294
Tel: 0035318962014
E-mail: tfoster@tcd.ie

(Received 8 February 2011, revised 19 April 2011, accepted 4 May 2011)

doi:10.1111/j.1742-4658.2011.08159.x

The fibronectin-binding proteins FnBPA and FnBPB are multifunctional adhesins than can also bind to fibrinogen and elastin. In this study, the N2N3 subdomains of region A of FnBPB were shown to bind fibrinogen with a similar affinity to those of FnBPA (2 μM). The binding site for FnBPB in fibrinogen was localized to the C-terminus of the γ-chain. Like clumping factor A, region A of FnBPB bound to the γ-chain of fibrinogen in a $Ca^{2+}$-inhibitable manner. The deletion of 17 residues from the C-terminus of domain N3 and the substitution of two residues in equivalent positions for crucial residues for fibrinogen binding in clumping factor A and FnBPA eliminated fibrinogen binding by FnBPB. This indicates that FnBPB binds fibrinogen by the dock–lock–latch mechanism. In contrast, the A domain of FnBPB bound fibronectin with $K_D$ = 2.5 μM despite lacking any of the known fibronectin-binding tandem repeats. A truncate lacking the C-terminal 17 residues (latching peptide) bound fibronectin with the same affinity, suggesting that the FnBPB A domain binds fibronectin by a novel mechanism. The substitution of the two residues required for fibrinogen binding also resulted in a loss of fibronectin binding. This, combined with the observation that purified subdomain N3 bound fibronectin with a measurable, but reduced, $K_D$ of 20 μM, indicates that the type I modules of fibronectin bind to both the N2 and N3 subdomains. The fibronectin-binding ability of the FnBPB A domain was also functional when the protein was expressed on and anchored to the surface of staphylococcal cells, showing that it is not an artifact of recombinant protein expression.

**Structured digital abstract**

- **Fibronectin** binds to **fnbB** by filter binding (View interaction)
- **Fibronectin** binds to **fnbB** by surface plasmon resonance (View Interaction 1, 2)

## Introduction

*Staphylococcus aureus* is a commensal of the moist squamous epithelium of the human anterior nares [1]. It is also an important opportunistic pathogen that can cause superficial skin infections, as well as invasive life-threatening conditions, such as septic arthritis and endocarditis [2]. The development of *S. aureus*

**Abbreviations**
ClfA, clumping factor A; El, elastin; Fg, fibrinogen; Fn, fibronectin; FnBP, fibronectin-binding protein; FnBR, fibronectin-binding repeat; GBD, gelatin-binding domain; MSCRAMMs, microbial surface components recognizing adhesive matrix molecules; rGST, recombinant glutathione-*S*-transferase; SPR, surface plasmon resonance.

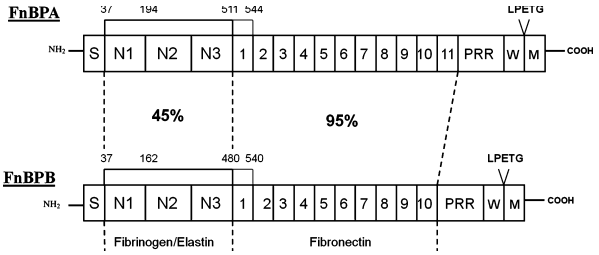


**Fig. 1.** Structural organization of fibronectin-binding proteins FnBPA and FnBPB from *Staphylococcus aureus* 8325-4. The N-termini of FnBPA and FnBPB contain a signal sequence (S) followed by a fibrinogen (Fg)- and elastin (El)-binding A domain consisting of subdomains N1, N2 and N3. Following the A domains are tandemly repeated fibronectin (Fn)-binding motifs (numbered). The A domains, as they were originally defined, contain a single Fn-binding motif. The true A domains of FnBPA and FnBPB comprise residues 37–511 and residues 37–480, respectively. At the C-termini are proline-rich repeats (PRR), wall (W)- and membrane (M)-spanning domains, and the sortase recognition motif LPETG. The percentage amino acid identities between the binding domains of FnBPA and FnBPB from *S. aureus* 8325-4 are shown. Figure reproduced from Ref. [10].

infections depends largely on the ability of the bacterium to adhere to components of the host's plasma and extracellular matrix via surface-expressed, ligand-binding proteins termed 'microbial surface components recognizing adhesive matrix molecules' (MSCRAMMs). These proteins act as virulence factors that allow *S. aureus* to adhere to the surface of host cells and to damaged tissue, and help it to avoid phagocytosis by neutrophils [3,4].

The fibronectin-binding proteins (FnBPs) A and B of *S. aureus* are multifunctional MSCRAMMs which recognize fibronectin (Fn), fibrinogen (Fg) and elastin (El) [5–7]. FnBPA and FnBPB have considerable organizational and sequence similarity and are composed of a number of distinct domains [5,8]. Figure 1 illustrates the domain organization of FnBPA and FnBPB of *S. aureus* strain 8325-4. Both proteins contain a secretory signal sequence at the N-terminus and a C-terminal LPETG motif required for sortase-mediated anchoring to cell wall peptidoglycan. The N-terminal A domains of FnBPA and FnBPB are exposed on the cell surface and promote binding to Fg and El. On the basis of their sequence similarity to the Fg-binding A domain of clumping factor A (ClfA), both FnBP A domains are predicted to fold into three subdomains: N1, N2 and N3 [9]. Seven isotypes of FnBPA and FnBPB have been identified on the basis of sequence variation in the N2 and N3 subdomains. Each recombinant isotype retains ligand-binding function, but is antigenically distinct [10,11].

The A domain of ClfA and FnBPA bind Fg at the C-terminus of the γ-chain [7]. The interaction between the A domain of ClfA and the γ-chain of Fg has been studied in detail. This interaction is inhibited by physiological concentrations of $Ca^{2+}$ ions which bind to the A domain of ClfA and induce a conformational change that is incompatible with binding [12]. The minimum ligand-binding site in the A domain of ClfA has been localized to subdomains N2 and N3 [9]. This region of ClfA has been crystallized in both the apo form and in a complex with a peptide corresponding to the C-terminus of the Fg γ-chain [13,14]. ClfA binds to the Fg γ-chain by a variation of the 'dock, lock and latch' mechanism, whereby the γ-chain peptide binds in a hydrophobic trench lying between the N2 and N3 subdomains [13,14]. ClfAs containing substitutions in residues P336 and Y338, which are located within the ligand-binding trench, were found to be defective in Fg binding [11,13]. On ligand binding, the C-terminal residues of domain N3 (latching peptide) undergo a conformational change forming an extra β-strand in N2. This traps the Fg peptide in the groove between N2 and N3 and locks it in place [13].

Previous work in our group has shown that, like ClfA, the N2 and N3 subdomains of FnBPA and FnBPB are sufficient for Fg binding and are predicted to bind to the γ-chain by a similar mechanism [10,15]. This is supported by structural models of the A domains of FnBPA and FnBPB which have a very similar conformation to the solved structure of ClfA, including the hydrophobic trench. Furthermore, residues N304 and F306 of FnBPA were found to be crucial for binding to Fg [15]. They are located in the equivalent positions to the aforementioned residues P336 and Y338 of ClfA. One of the objectives of this study was to determine the mechanism of Fg binding by the A domain of FnBPB.

Located distal to the A domains of FnBPA and FnBPB are multiple tandemly arranged Fn-binding repeats (FnBRs) which mediate binding to the N-terminal type I modules of Fn by a tandem β-zipper mechanism [16]. The Fn-binding moiety is organized into 11 tandem repeats, each capable of interacting with the N-terminal domains of Fn, whereas FnBPB contains 10 rather than 11 repeats [17] (Fig. 1). The binding of Fn is critical for the invasion into non-phagocytic host cells. It acts as a molecular bridge linking the bacterial cell to the host integrin $\alpha_5\beta_1$ [3]. The subsequent internalization of *S. aureus* protects the bacterium from the host immune system and promotes its spread from the site of infection to other tissues and organs of the host. Indeed, FnBP-mediated invasion of endothelial and epithelial cells is an

important virulence factor in animal models of endocarditis [18,19].

The co-ordinates of FnBPA and FnBPB from *S. aureus* strain 8325-4 have been redefined recently [17] (Fig. 1). We have demonstrated that residues 194–511 of FnBPA promote binding only to immobilized Fg and El, confirming the absence of any Fn-binding motifs in the revised N2N3 subdomain [15,17]. By contrast, residues 163–480 of FnBPB promote binding to Fg, El and Fn with similar affinities [10]. This raises the possibility that, unlike FnBPA, the A domain of FnBPB contains a novel Fn-binding motif and may bind Fn by a novel mechanism. The aim of this study was to determine whether Fg and Fn bind to the A domain of FnBPB by distinct mechanisms and to localize the binding sites for the A domain of FnBPB in Fn.

## Results

### Binding of the full-length FnBPB A domain to immobilized Fg

It has been reported previously that FnBPB A domain residues 163–480, comprising subdomains N2 and N3, promote binding to immobilized Fg [10]. It has been proposed that, like FnBPA and ClfA, the N1 subdomain of FnBPB plays no role in the interaction between FnBPB and Fg. To determine whether the N1 subdomain plays any role in the binding, a recombinant protein comprising subdomains N1, N2 and N3 of FnBPB from *S. aureus* strain 8325-4 (residues 37–480) was expressed and purified. The affinity of $rFnBPB_{37–480}$ for Fg was measured using surface plasmon resonance (SPR). $rFnBPB_{37–480}$ bound dose dependently to Fg with an affinity constant ($K_D$) of $2 \pm 0.86$ μM. This is identical to the affinity constant calculated previously for the interaction between the N2N3 subdomain of FnBPB (residues 163–480) and Fg [10]. A representative sensorgram is shown in Fig. 2. These data indicate that the N1 subdomain of FnBPB (residues 37–162) plays no role in Fg binding *in vitro*.

### Effects of cations on the interaction between ClfA and the Fg γ-chain

Previous studies with ClfA have indicated that the physiological concentration of $Ca^{2+}$ ions (~ 2.5 mM) partially inhibits the interaction between ClfA and Fg [12]. In this study, the possible effect of divalent cations on the interaction between $rFnBPB_{163–480}$ and Fg was analysed by SPR. As Fg is known to be a

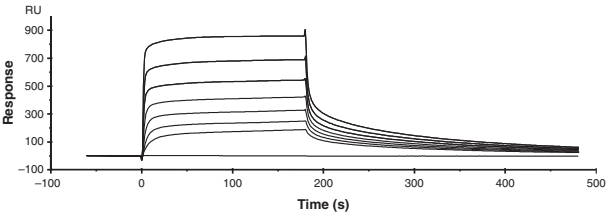


**Fig. 2.** Surface plasmon resonance analysis of $rFnBPB_{37–480}$ binding to fibrinogen (Fg). Human Fg was immobilized onto the surface of a dextran chip. $rFnBPB_{37–480}$ was passed over the surface in concentrations ranging from 0.15 (lowermost trace) to 20 μM (uppermost trace). The sensorgram has been corrected for the response obtained when $rFnBPB_{37–480}$ was passed over uncoated chips, and is representative of three independent experiments.

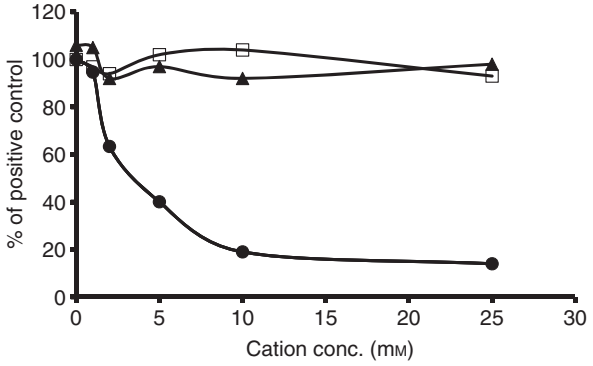


**Fig. 3.** Inhibition of $rFnBPB_{163–480}$ binding to fibrinogen (Fg) by $Ca^{2+}$ ions. $rFnBPB_{163–480}$ (1 μM) was incubated with increasing concentrations of $CaCl_2$ (●), $MgCl_2$ (□) or $NiCl_2$ (▲) at room temperature for 1 h before being passed over the surface of a recombinant glutathione-*S*-transferase (rGST) γ-chain-coated chip. Maximum binding levels (RU) are expressed as a percentage of a cation-free $rFnBPB_{163–480}$ control sample. The graph is representative of three independent experiments.

$Ca^{2+}$-binding protein, we chose to use a recombinant glutathione-*S*-transferase (rGST)-tagged, C-terminal Fg γ-chain peptide as the ligand and to assume that the observed effects of metal ions would reflect interactions between Fg and FnBPB. Samples of $rFnBPB_{163–480}$ were incubated with increasing concentrations of $CaCl_2$, $MgCl_2$ or $NiCl_2$ and passed over the surface of an rGST γ-chain-coated chip. The maximum binding level (RU) reached by each sample was calculated as a percentage of the maximum binding level reached by a cation-free control sample of $rFnBPB_{163–480}$. The presence of $Ca^{2+}$ ions inhibited the binding of $rFnBPB_{163–480}$ in a dose-dependent manner, whereas the presence of $Mg^{2+}$ or $Ni^{2+}$ ions had no effect (Fig. 3). The binding of $rFnBPB_{163–480}$ to rGST γ-chain was inhibited by 50% at a $Ca^{2+}$ concentration of 2.5 mM. This is

similar to the concentration of $Ca^{2+}$ that is present in normal human sera. These data show that, like ClfA and FnBPA, FnBPB binds to the C-terminus of the γ-chain of Fg. The results also suggest that, like ClfA, $Ca^{2+}$ ions bind to an inhibitory site within the A domain of FnBPB.

## Ligand binding by rFnBPB N2N3 lacking C-terminal residues

One objective of this project was to determine whether the A domain of FnBPB binds Fg by the same mechanism as the A domain of ClfA. A three-dimensional molecular model of the N2N3 domains of FnBPB based on the known structure of ClfA has been constructed previously [10]. Based on this model, the C-terminal 17 residues of the N3 subdomain of FnBPB were deleted (Fig. 4). In the crystal structure of ClfA, these residues form the latching peptide that plays a crucial role in the dock, lock and latch mechanism of ligand binding. As FnBPB is predicted to bind to the Fg γ-chain by the same mechanism, it was proposed that the C-terminal 17 residues of the A domain of FnBPB form the latching peptide and play a similar role in the interaction of FnBPB with Fg. To test this hypothesis, a recombinant truncate of the FnBPB N2N3 protein, which lacked the predicted latching peptide ($rFnBPB_{163–463}$), was expressed and its ability to bind to immobilized Fg was analysed by SPR using the same Fg-coated chips. No detectable interaction was observed when concentrations of $rFnBPB_{163–463}$ of 0.15–20 μM were passed over the surface of the Fg-coated chips (Fig. 5A). This indicates that the C-terminal 17 residues of the A domain of FnBPB are essential for the interaction of FnBPB with Fg, and may be important for the 'latching' and 'locking' steps in the Fg-binding mechanism.

Residues 163–480 of FnBPB do not contain any known Fn-binding motifs. However, when the binding ability of $rFnBPB_{163–480}$ was tested previously, the protein was found to bind to both immobilized Fg and Fn dose dependently and with similar affinities [10]. Another objective of this study was to determine whether the N2N3 subdomain of FnBPB binds Fg and Fn by different mechanisms. The interaction of the C-terminal truncate $rFnBPB_{163–463}$ with Fn was analysed by SPR and bound dose dependently to Fn with an affinity constant ($K_D$) of 2 ± 0.71 μM (Fig. 5B). This is very similar to the $K_D$ value for the full-length wild-type protein $rFnBPB_{163–480}$ (2.5 μM) [10]. This indicates that C-terminal residues of the N2N3 subdomain of FnBPB play no role in the Fn-binding mechanism,

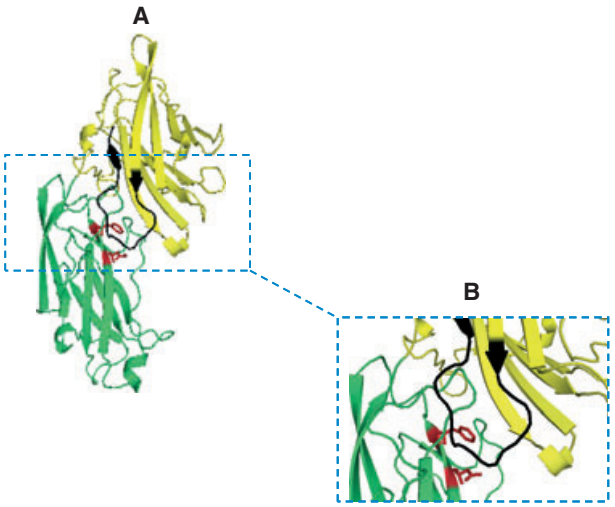


**Fig. 4.** Three-dimensional structural model of FnBPB N2N3. (A) Based on the crystal structure of domain A of clumping factor A (ClfA), a ligand-binding trench is predicted to form between the N2 (green) and N3 (yellow) domains of FnBPB. The 17 C-terminal residues that are predicted to form the putative latching peptide are shown in black. Residues N312 and F314, which were selected for alteration by site-directed mutagenesis, are shown in red ball and stick form and are enlarged in (B).

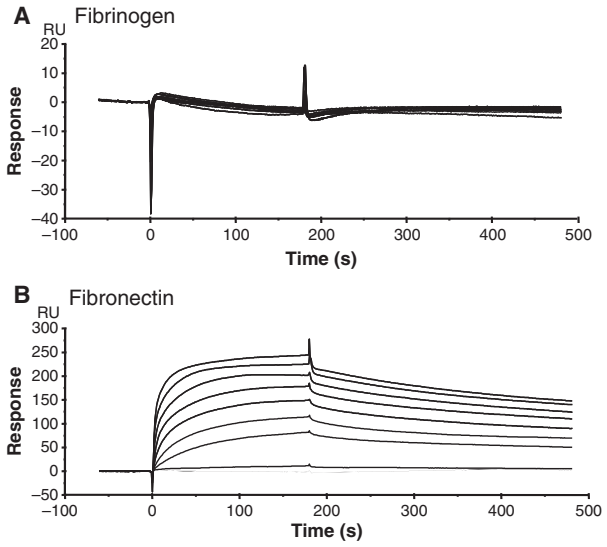


**Fig. 5.** Surface plasmon resonance analysis of $rFnBPB_{163–463}$ binding to fibrinogen (Fg) and fibronectin (Fn). Human Fg (A) or Fn (B) was immobilized onto the surface of a dextran chip. $rFnBPB_{163–463}$ was passed over the surface in concentrations ranging from 0.15 (lowermost trace) to 20 μM (uppermost trace). The representative sensorgrams have been corrected for the response obtained when $rFnBPB_{163–466}$ was passed over uncoated chips, and each is representative of three independent experiments.

and suggest that different mechanisms are involved in the binding of the A domain of FnBPB to the two ligands.

## Ligand binding by rFnBPB N2N3 N312A/F314A

In order to investigate whether FnBPB binds Fg by the same mechanism as ClfA and FnBPA, amino acids in the equivalent positions to residues previously shown to be important in Fg binding were chosen for alteration. Residues N312 and F314 of FnBPB are predicted to line the putative ligand-binding trench in positions equivalent to P336 and Y338 of ClfA, and N304 and F306 of FnBPA (Fig. 4). These residues were altered to form $rFnBPB_{163–480}$ N312A/F314A. The interaction between $rFnBPB_{163–480}$ N312A/F314A and Fg was analysed by SPR. No reliable kinetic parameters could be obtained when concentrations of $rAFnBPB_{163–480}$ N312A/F314A ranging from 0.15 to 20 μM were passed over the surface of the chip (data not shown), showing that the residues are involved in the interaction between $rFnBPB_{163–480}$ and Fg. To investigate this further, equal amounts of $rFnBPB_{163–480}$ N312A/F314A and wild-type $rFnBPB_{163–480}$ were passed over the surface of an Fg-coated chip and the level of binding was compared. The mutant showed greatly reduced binding (Fig. 6A). The maximum was 190 RU, compared with the wild-type protein which reached a maximum of 800 RU. These results indicate that residues N312 and F314 of the A domain play an important role in the interaction of FnBPB with Fg. They are predicted to be located within the ligand-binding trench and may therefore play an important role in the 'docking' step of Fg binding.

In order to determine whether the predicted ligand-binding trench plays a role in the interaction between the A domain of FnBPB and Fn, the binding of $rFnBPB_{163–463}$ N312A/F214A to immobilized Fn was also analysed by SPR. Equal amounts of $rFnBPB_{163–480}$ N312A/F314A and wild-type $rFnBPB_{163–480}$ were passed over the surface of an Fn-coated chip. The maximum binding level reached by the mutant protein was 25 RU, whereas the wild-type protein reached a maximum of 55 RU (Fig. 6B), indicating that residues N312 and F314 play an important role in the binding of the A domain of FnBPB to Fn.

## Binding of rFnBPB N2 and rFnBPB N3 to immobilized Fn

In order to localize the Fn-binding site in the N2N3 subdomain of FnBPB, the recombinant FnBPB N2 ($rFnBPB_{163–308}$) and N3 ($rFnBPB_{309–480}$) subdomains were tested for binding to Fn by SPR. Equal amounts of $rFnBPB_{163–308}$, $rFnBPB_{309–480}$ and wild-type $rFnBPB_{163–480}$ were passed over the surface of an Fn-coated chip. Both individual recombinant subdomains showed greatly reduced binding to Fn when compared with the wild-type rN2N3 protein, which reached a maximum binding level of 95 RU (Fig. 7A). Although $rFnBPB_{163–308}$ reached a maximum binding level of 12 RU, $rFnBPB_{309–480}$ reached a significantly higher level of 52 RU (Fig. 8B). $rFnBPB_{309–480}$ bound to immobilized Fn with an affinity constant ($K_D$) of 22.7 μM (Fig. 8B), approximately 10-fold weaker than the affinity constant for the wild-type $rFnBPB_{163–480}$ (2.5 μM) [10]. An even weaker reaction was observed with $rFnBPB_{163–308}$ (data not shown) and no reliable kinetic parameters could be obtained. These results suggest that both subdomains N2 and N3 play a role in the interaction between the N2N3 region of FnBPB and Fn.

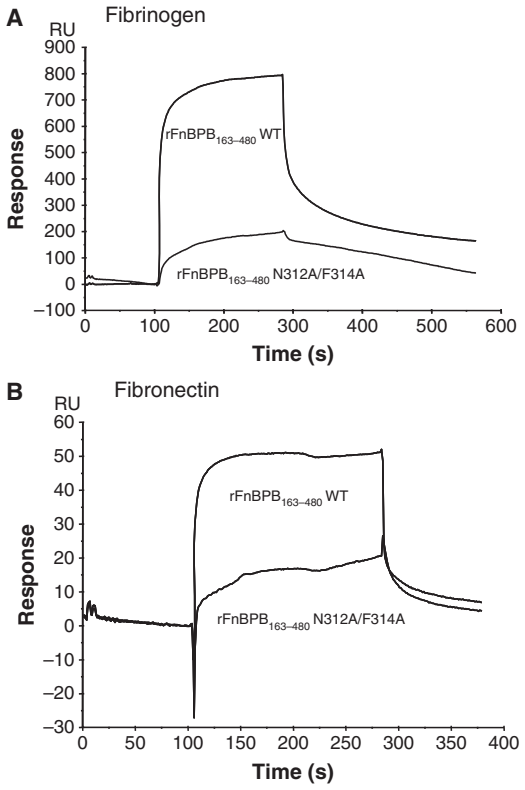


**Fig. 6.** Surface plasmon resonance analysis of $rFnBPB_{163–480}$ N312A/F314A binding to fibrinogen (Fg) and fibronectin (Fn). Equal amounts of $rFnBPB_{163–480}$ N312A/F314A (lowermost traces) and wild-type (WT) (uppermost traces) protein were passed over the surface of the same Fg (A) or Fn (B) chip. The sensorgrams have been corrected for the response obtained when recombinant FnBPB proteins were passed over uncoated chips, and each is representative of three independent experiments.

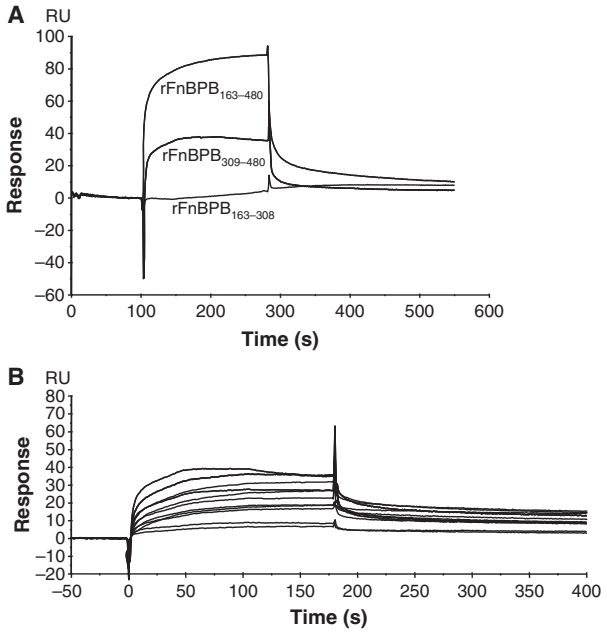


**Fig. 7.** Surface plasmon resonance analyses of $rFnBPB_{163–308}$ and $rFnBPB_{309–480}$ binding to fibronectin (Fn). (A) Equal amounts (2 μM) of $rFnBPB_{163–480}$ (top trace), $rFnPBB_{163–308}$ (bottom trace) and $rFnBPB_{309–480}$ (middle trace) were passed over the surface of the same Fn-coated chip. (B) Concentrations of $rFnBPB_{309–480}$ ranging from 0.15 to 20 μM were passed over the surface of an Fn-coated chip. Each sensorgram has been corrected for the response obtained when recombinant FnBPB proteins were passed over uncoated chips, and is representative of three independent experiments.

## Binding of rFnBPB N2N3 to immobilized Fn fragments

The binding site in Fn for *S. aureus* FnBPs is located in the N-terminus [20]. However, another binding site in the C-terminal gelatin-binding domain (GBD) has also been reported [21,22]. The C-terminal FnBRs of *S. aureus* FnBPs promote binding to the N-terminal F1 modules of Fn. To localize the binding site in Fn for the N2N3 subdomain of FnBPB, the binding of $rFnBPB_{163–480}$ to different fragments of Fn was tested. These fragments included a 29-kDa fragment containing the five N-terminal Type 1 modules (N29) and C-terminal fragments GBD, 607–1265, 1266–1908 and 1913–2477 (Fig. 8A). $rFnBPB_{163–480}$ bound to whole Fn and to the N29 fragment with similar affinities (Fig. 8B). By contrast, $rFnBPB_{163–480}$ reacted poorly with Fn fragments GBD, 607–1265, 1266–1908 and 1913–2477. This indicates that the binding site in Fn for the N-terminal A domain of FnBPB is localized to the same region of Fn to which the C-terminal FnBRs of FnBPB bind.

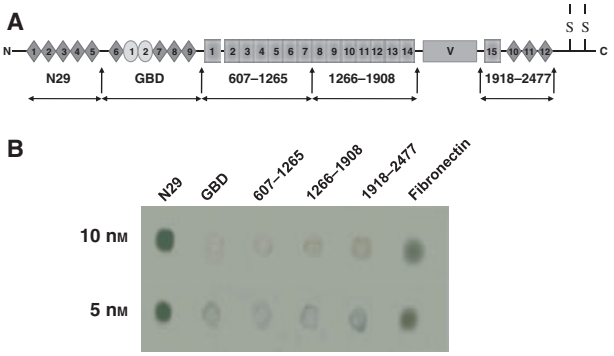


**Fig. 8.** Binding of $rFnBPB_{163–480}$ to fibronectin (Fn) and Fn fragments by dot immunoblotting. (A) Fn is shown as a monomer and is composed of three different types of protein module: F1, F2 and F3. The variably spliced V region is shown. Thermolysin cut sites are indicated by arrows. The N-terminal 29-kDa fragment (N29), gelatin-binding fragment (GBD) and fragments 607–1265, 1266–1908 and 1913–2477 were used in this study and are labelled. (B) Equal amounts (10 or 5 nM) of whole Fn and Fn fragments N29, BCD, 607–1265, 1266–1908 and 1913–2477 were applied to nitrocellulose membranes and probed with 1 $\mu g \cdot mL^{-1}$ $rFnBPB_{163–480}$. Bound recombinant protein was detected using polyclonal anti-rFnBPB serum followed by horseradish peroxidase-conjugated goat anti-rabbit IgG.

## The A domain of FnBPB promotes bacterial adhesion to immobilized Fn

To investigate the biological significance of Fn binding by the A domain of FnBPB, it was important to determine whether the A domain alone could promote bacterial adhesion to the ligand. This required expression of the N-terminal A domain of FnBPB in the absence of the C-terminal FnBRs on the bacterial cell surface. To facilitate this, shuttle plasmid p*fnbA*::R*clfA* was constructed, which expressed a chimeric protein containing the A domain of FnBPB together with region R and the cell wall anchoring region of *S. aureus* ClfA (Fig. 9A). Region R of ClfA has no known ligand-binding function. It consists of a series of serine–aspartate repeats that project the ligand-binding A domain away from the cell surface, allowing interaction with Fg [23].

The expression of the chimeric FnBPBA-RClfA protein on the surface of the surrogate host *S. epidermidis* promoted dose-dependent and saturable adhesion to Fg, El and Fn (Fig. 9). *Staphylococcus epidermidis* cells expressing the chimeric FnBPBA-RClfA protein or wild-type FnBPB adhered with similar affinities to Fg-coated and El-coated wells (Fig. 9B, i and ii). This demonstrates the functionality of the N-terminal A domain of the chimeric protein. By contrast, the affinity of *S. epidermidis* cells expressing the chimeric

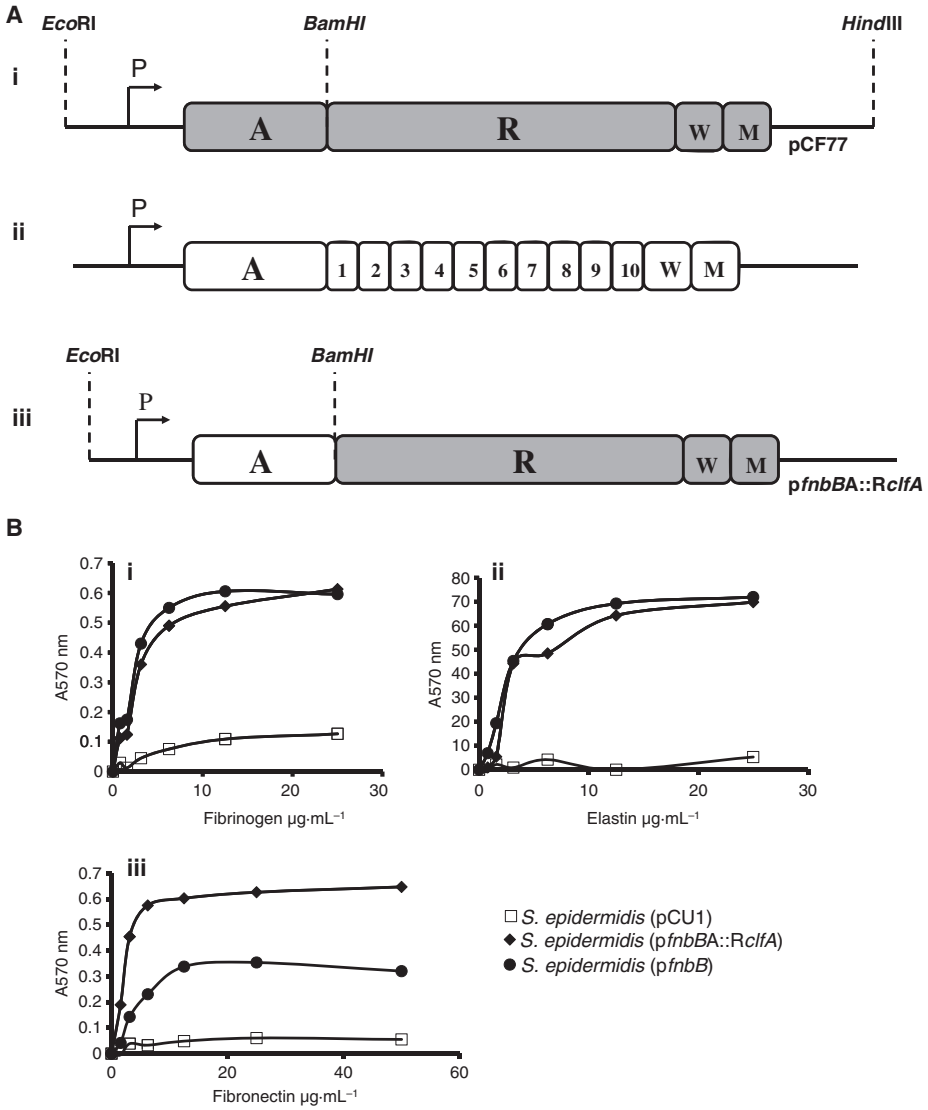


**Fig. 9.** Adherence of *Staphylococcus epidermidis* strains expressing full-length FnBPB or chimeric FnBPBA::RClfA to immobilized ligands. (A) Construction of plasmids p*fnbB*A::R*clfA*. DNA encoding the fibrinogen (Fg)-binding A domain of clumping factor A (ClfA) and upstream promoter region is contained within a 3-kb *EcoRI-BamHI* fragment of pCF77 (i). A 1.9-kb fragment encoding the A domain of FnBPB and upstream promoter region (ii) was cloned between the *Eco*RI and *Bam*HI sites of pCF77 to produce p*fnbB*A::R*clfA* (iii). pCU1-*fnbB* was used as a control. (B) Adherence of *S. epidermidis* strains to immobilized ligands. *Staphylococcus epidermidis* expressing full-length FnBPB, chimeric FnBPBA::RClfA or carrying empty vector (pCU1) was grown to exponential phase. Washed cell suspensions were added to ligand-coated microtitre wells and allowed to adhere. Bacterial adherence to Fg (i) and fibronectin (Fn) (iii) was measured by staining with crystal violet, and elastin (El) adherence (ii) was measured using SYTO-13 fluorescent dye. Data points represent the mean of triplicate wells. Each graph is representative of three independent experiments.

FnBPBA::RClfA protein for Fn was considerably weaker than that of cells expressing full-length FnBPB (Fig. 9B, iii). These results suggest that the C-terminal FnBRs of FnBPB are necessary to promote high-affinity bacterial adherence to Fn, whereas lower adherence was achieved by the expression of the ligand-binding site in the A domain of FnBPB.

## Discussion

An important factor in bacterial pathogenesis is the ability of the invading organism to colonize host tissue. *Staphylococcus aureus* possesses on its cell surface a family of adhesion proteins, known as MSCRAMMs, which promote the binding of the

organism to components of the host's plasma and extracellular matrix. The Fn-binding proteins FnBPA and FnBPB are multifunctional MSCRAMMs that interact specifically with Fg, El and Fn. Ligand binding by *S. aureus* FnBPs has been shown to promote platelet activation and aggregation, as well as internalization into host cells [4,24]. The expression of FnBPs is an important virulence factor in the animal models for endocarditis and septic arthritis [19,25].

The N-terminal A domains of ClfA, FnBPA and FnBPB each promote binding to the C-terminus of the γ-chain of Fg [7]. They share a similar structural organization, consisting of subdomains N1, N2 and N3, and are predicted to bind Fg by a similar mechanism. Previous studies from our group have indicated that the N2N3 subdomain of FnBPB (residues 163–480) is sufficient for binding to immobilized Fg [10]. Here, a recombinant N1N2N3 construct spanning residues 37–480 was created to assess the function of N1 in ligand binding. $rFnBPB_{37–480}$ and $rFnBPB_{163–480}$ bound Fg with identical $K_D$ values, indicating that the N1 subdomain does not have any role in Fg binding. This is in accordance with the A domains of ClfA and FnBPA, the N2N3 subdomains of which contain the minimal binding site for Fg [13,15].

The three-dimensional structures of the N2N3 subdomains of SdrG and ClfA have greatly increased our understanding of the mechanisms by which they bind to peptide ligands. A dynamic mechanism has been proposed, called 'dock, lock and latch' [26]. Sequence analysis has indicated that structurally related ligand-binding regions from the A domains of ClfA, FnBPA and FnBPB share conserved motifs which include a potential latching peptide [26], and that the dock, lock and latch mechanism is common to these proteins.

The C-terminal residues 464–480 are predicted to form the latching peptide. This hypothesis was tested by constructing a truncate of the N2N3 protein ($rFnBPB_{163–463}$) which lacked the predicted latching peptide. $rFnBPB_{163–463}$ did not bind detectably to Fg, indicating that, like ClfA and FnBPA, the C-terminal residues of the N3 subdomain are crucial, providing evidence for the dock, lock and latch mechanism.

To define further the Fg-binding site in FnBPB, amino acids were chosen for alteration as a result of their equivalent positions to residues previously shown to be important for Fg binding by ClfA and FnBPA. Residues N312 and F314 were predicted to line the ligand-binding trench in positions equivalent to P336 and Y338 of ClfA and N304 and F306 of FnBPA, respectively. The substitution of residues N312 and F314 dramatically reduced the affinity of $rFnBPB_{163–480}$ for Fg, indicating that they play an important role in Fg binding. This provides further evidence that Fg binds to ClfA, FnBPA and FnBPB in a similar manner. Taken together, these data highlight the structural similarities between the A domains of ClfA, FnBPA and FnBPB.

The interaction between the A domain of ClfA and the γ-chain of Fg is inhibited by micromolar concentrations of $Ca^{2+}$ ions, which bind to the A domain and induce a conformational change that is incompatible with binding [12]. As ClfA and FnBPB are predicted to bind to the Fg γ-chain in a similar manner, it was proposed here to test whether the A domain of FnBPB also contains an inhibitory binding site for $Ca^{2+}$ ions. As with ClfA, physiological concentrations of $Ca^{2+}$ inhibited the binding of $rFnBPB_{163–480}$. ClfA is predominantly expressed during the stationary phase of growth [12]. As *S. aureus* FnBPs are expressed exclusively during the exponential phase, it may be that $Ca^{2+}$-dependent regulation of FnBP activity prevents some of the Fg receptors in this phase from being occupied by soluble Fg. This may allow *S. aureus* cells to adhere to solid-phase Fg or fibrin clots during the early growth phase and may allow cells to detach from the vegetations and spread.

The Fg-binding A domains of FnBPA and FnBPB are followed by intrinsically disordered C-terminal regions containing 11 (FnBPA) or 10 (FnBPB) non-identical FnBRs. They bind to the N-terminal domain of Fn by the tandem β-zipper mechanism [15–17]. The N2N3 subdomains of FnBPA and FnBPB span residues 194–511 and residues 163–480, respectively, and do not include any FnBR sequences [15,17]. $rFnBPB_{163–480}$ unexpectedly bound to both immobilized Fg and Fn with similar affinities [10]. This raised the possibility that, unlike FnBPA, the A domain of FnBPB contains a novel Fn-binding motif that may bind Fn by a novel mechanism.

To investigate this, rFnBPB N2N3 mutants that were defective in Fg binding were tested for their ability to bind Fn. Deletion of the predicted latching peptide, which is essential for Fg binding, had no affect on the affinity of rFnBPB N2N3 for Fn, indicating that FnBPB binds the ligands by distinct mechanisms. The substitution of FnBPB residues N312 and F314 reduced the affinity of rFnBPB N2N3 for Fg and also reduced binding to Fn. This suggests that residues in the ligand-binding trench of FnBPB play a key role in both the Fg- and Fn-binding mechanisms. The N3 subdomain alone showed a reduced, but measurable, affinity for Fn, suggesting that it carries a significant part of the Fn-binding site. Residues N312 and F314 are part of subdomain N2, which suggests that Fn binds to both subdomains N2 and N3.

To localize the binding site in Fn, the binding of rFnBPB N2N3 to different fragments of Fn was tested. The recombinant protein bound with similar affinity to whole Fn and to an N-terminal fragment of Fn containing F1 modules 1–5. This is the same region of Fn with which the C-terminal FnBRs of FnBPA and FnBPB interact. Binding of the type 1 Fn modules to the C-terminal FnBRs triggers the uptake of *S. aureus* by human endothelial cells and is believed to facilitate *S. aureus* persistence and the establishment of secondary (metastatic) infections. Several high-affinity FnBRs occur within FnBPA (1–44 nM), and at least one is required for the uptake of *S. aureus* by endothelial cells. The lower affinity FnBRs alone are not sufficient [17,27]. It is therefore unlikely that low-affinity Fn binding by the A domain of FnBPB (2.5 μM) is sufficient to promote the bacterial invasion of endothelial cells.

To explore the biological significance of the interaction between the A domain of FnBPB and Fn, the ability of the A domain, in isolation from FnBRs, to promote bacterial adhesion to Fn was examined by constructing a chimeric FnBPBA-RClfA protein containing the A domain of FnBPB and the stalk and cell wall anchoring region of ClfA. The protein promoted dose-dependent and saturable adhesion of *S. epidermidis* to Fg, El and Fn. This supports the conclusions from studies with the recombinant protein and confirms that the A domain of FnBPB contains a binding site for Fn. The affinity for Fn of *S. epidermidis* cells expressing FnBPBA-RClfA was significantly weaker than that of cells expressing full-length wild-type FnBPB with its full complement of FnBRs. Nevertheless, the low-affinity interaction with Fn must play an important role *in vivo* because binding is retained in the seven antigenically distinct isotypes of FnBPB [10].

## Experimental procedures

### Bacterial strains and growth conditions

Cloning was routinely performed in *Escherichia coli* strain XL-1 Blue (Stratagene, La Jolla, CA, USA). *Escherichia coli* strains were transformed by the calcium chloride method [28]. *Escherichia coli* strain TOPP 3 (Qiagen, Madison, WI, USA) was used for the expression of recombinant FnBPB A domain proteins. Ampicillin (100 $\mu g \cdot mL^{-1}$) was incorporated into growth media where appropriate. *Staphylococcus epidermidis* strain TU3298 [29] was used to carry empty vector (pCU1) [30] or for heterologous cell surface expression of full-length FnBPB (p*fnbB*) or FnBPBA-RClfA chimeric protein (p*fnbB*A::R*clfA*). *Staphylococcus epidermidis* was routinely grown on trypticase soy agar (Oxoid, Cambridge, UK) or trypticase soy broth at 37 °C for liquid cultures. Chloramphenicol (10 $\mu g \cdot mL^{-1}$) was incorporated into trypticase soy broth where appropriate.

### Genetic techniques

Plasmid DNA (Table 1) was isolated using the Wizard® Plus SV Miniprep Kit (Promega, Madison, WI, USA), according to the manufacturer's instructions, and finally transformed into *E. coli* XL-1 Blue cells using standard procedures [28]. Transformants were screened by restriction analysis and verified by DNA sequencing (GATC Biotech, Konstanz, Germany). Chromosomal DNA was extracted using the Bacterial Genomic DNA Purification Kit (Edge Biosystems, Gaithersberg, MD, USA). Restriction digests and ligations were carried out using enzymes from New England Biolabs (Ipswich, MA, USA) and Roche (Basel, Switzerland), according to the manufacturers' protocols. Oligonucleotides were purchased from Sigma Aldrich, Dublin, Ireland and are listed in Table 2. DNA purification was carried out using the Wizard® SV Gel and PCR Clean-up System (Promega).

### Construction of a chimeric FnBPBA-RClfA protein

Shuttle plasmid pCF77 has been described previously [23]. It carries the entire *clfA* gene from strain 8325-4 together with 1300 bp of upstream sequence containing the *clfA* promoter region. pCF77 DNA was cleaved with *Eco*RI and *Bam*HI to remove DNA encoding the Fg-binding A domain of ClfA and upstream promoter region, which is contained within a 3-kb *Eco*RI-*Bam*HI fragment of the plasmid. Primers $FnBPB_{(142–480)}$ F and $FnBPB_{(142–480)}$ R were designed to amplify 1.9 kb of *fnbB* DNA from strain 8325-4 genomic DNA, which encodes the entire A domain of FnBPB and contains the upstream *fnbB* promoter. The PCR product was cleaved with *Eco*RI and *Bam*HI at restriction sites incorporated into the primers, and ligated to pCF77 DNA cleaved with the same enzymes to generate plasmid p*fnb*BA::R*clf*A for the expression of a chimeric protein containing the A domain of FnBPB and the stalk (region R) and cell wall anchoring domain of ClfA (Fig. 9A).

Primers $FnBPB_{(388–980)}$ F and $FnBPB_{(388–980)}$ R were designed to amplify DNA encoding FnBPB residues 388–980 using genomic DNA from strain 8325-4 as a template. The PCR product was cleaved with *Hind*III at restriction sites incorporated into the primers and ligated to p*fnbB*A::R*clfA* DNA cleaved with the same enzyme to generate plasmid p*fnb*B for the expression of full-length wild-type FnBPB.

### Three-dimensional model for FnBPB N2N3

A theoretical three-dimensional model of the N2N3 subdomain of FnBPB (residues 163–480) has been described previously [10]. The protein structure file was viewed using

**Table 1.** Plasmids.

| Plasmid | Features | Marker(s) | Source/reference |
|---|---|---|---|
| pQE30 | *E. coli* vector for the expression of hexa-His-tagged recombinant proteins | $Amp^R$ | Qiagen |
| pQE30::rFnBPB$_{163–480}$ | pQE30 derivative encoding the N2N3 subdomain of FnBPB from *S. aureus* 8325-4 | $Amp^R$ | [10] |
| pQE30::rFnBPB$_{37–480}$ | pQE30 derivative encoding residues of the full-length A domain (N1N2N3) of FnBPB from *S. aureus* 8325-4 | $Amp^R$ | This study |
| pQE30::rFnBPB$_{163–463}$ | pQE30 derivative encoding residues 163–463 of FnBPB from *S. aureus* 8325-4 | $Amp^R$ | This study |
| pQE30::rFnBPB$_{163–308}$ | pQE30 derivative encoding residues 163–308 (subdomain N2) of FnBPB from *S. aureus* 8325-4 | $Amp^R$ | This study |
| pQE30::rFnBPB$_{309–480}$ | pQE30 derivative encoding residues 309–480 (subdomain N3) of FnBPB from *S. aureus* 8325-4 | $Amp^R$ | This study |
| pQE30::rFnBPB$_{163–480}$ N312A/F314A | pQE30 derivative encoding the N2N3 subdomain of FnBPB from *S. aureus* 8325-4 with mutations encoding the changes N312A and F314A | $Amp^R$ | This study |
| pCU1 | Derivative of pC194 and pUC19. Shuttle vector | $Amp^R$ in *E. coli* $Cm^R$ in *S. epidermidis* | [30] |
| pCF77 | pCU1 derivative containing an entire copy of the *clfA* gene | $Amp^R$ in *E. coli* $Cm^R$ in *S. epidermidis* | [23] |
| pCU1*fnbB* | pCU1 derivative containing an entire copy of the *fnbB* gene | $Amp^R$ in *E. coli* $Cm^R$ in *S. epidermidis* | This study |
| p*fnbB*A::R*clfA* | pCF77 derivative encoding chimeric protein FnBPBA::RClfA | $Amp^R$ in *E. coli* $Cm^R$ in *S. epidermidis* | This study |

**Table 2.** Primers.

| Primer | Sequence (5′–3′)[a,b] | 5′ restriction site |
|---|---|---|
| rFnBPB$_{37–480}$ F | CGG*GGATCC*GCATCGGAACAAAACAATAC | *Bam*HI |
| rFnBPB$_{37–480}$ R | AAT*CCCGGG*TTACTTTAGTTTATCTTTGCCG | *Sma*I |
| rFnBPB$_{163–463}$ F | GGG*GGATCC*GGTACAGATGTAACAAATAAAG | *Bam*HI |
| rFnBPB$_{163–463}$ R | ATT*CCCGGG*TAATTTTTCCAAGTTAAATTACTTG | *Sma*I |
| rFnBPB$_{163–308}$ F | GGG*GGATCC*GGTACAGATGTAACAAATAAAG | *Bam*HI |
| rFnBPB$_{163–308}$ R | CTC*CCCGGG*CTATTGAATATTAAATATTTTGCTAA | *Sma*I |
| rFnBPB$_{309–480}$ F | CCC*GGATCC*TATTTAGGTGGAGTTAGAGATAAT | *Bam*HI |
| rFnBPB$_{309–480}$ R | AAT*CCCGGG*TTACTTTAGTTTATCTTTGCCG | *Sma*I |
| rFnBPB$_{163–480}$ NF F | GAATTATCTTTA**GC**TCTA**GC**TATTGATCC | |
| rFnBPB$_{163–480}$ NF F | GGATCAATA**GC**TAGA**GC**TAAAGATAATTC | |
| FnBPB$_{(–142–480)}$ F | GCA*GAATTC*GTCGGCTTGAAATACGCTG | *Eco*RI |
| FnBPB$_{(–142–480)}$ R | AAT*GGATCC*TTACTTTAGTTTATCTTTGCCG | *Bam*HI |
| FnBPB$_{(388–980)}$ F | CCC*AAGCTT*GATGATGTCAGC | *Hind*III |
| FnBPB$_{(388–980)}$ R | CCC*AAGCTT*GAACGCCTTCATAGTGTC | *Hind*III |

[a] Restriction sites used for cloning are shown in italic. [b] Nucleotides changed for site-directed mutagenesis are indicated in bold.

PYMOL viewing software (http://pymol.sourceforge.net/) for the rational design of recombinant FnBPB A domain mutants.

## Expression and purification of recombinant proteins

Regions of the *fnbB* gene encoding amino acids 37–480, 163–463, 163–308 and 309–480 were PCR amplified from *S. aureus* 8325-4 genomic DNA using primers incorporating *Bam*HI and *Sma*I restriction sites. The PCR products were cloned into the N-terminal six-His tag expression vector pQE30 (Qiagen). pQE30 containing the *S. aureus* 8325-4 *fnbB* DNA sequence encoding amino acids 163–480 [10] was subjected to site-directed mutagenesis by the Quick-change method (Stratagene). Complementary primers, each containing the desired nucleotide changes, were extended during thermal cycling, creating a mutated plasmid which was digested with *Dpn*I and then transformed into *E. coli* XL-1

Blue. Recombinant proteins were purified by $Ni^{2+}$ chelate chromatography [12]. Protein concentrations were determined using the BCA Protein Assay Kit (Pierce Biotechnology, Rockford, IL, USA). Proteins were dialysed against NaCl/$P_i$ for 24 h at 4 °C, aliquoted and stored at –70 °C.

### SPR analysis of rFnBPB proteins binding to immobilized ligands

SPR was performed using the BIAcore X100 system (GE Healthcare, Amersham, UK). Human Fg (Calbiochem, Nottingham, UK), Fn (Calbiochem) and rGST γ-chain (a gift from Dr Joan Geoghegan, Trinity College, Dublin, Ireland) were covalently immobilized on CM5 sensor chips using amine coupling. This was performed using 1-ethyl-3-(3-dimethylaminopropyl) carbodiimide hydrochloride, followed by *N*-hydroxysuccinimide and ethanolamine hydrochloride, as described by the manufacturer. Fg (50 $\mu g \cdot mL^{-1}$), Fn (50 $\mu g \cdot mL^{-1}$) and rGST γ-chain (50 $\mu g \cdot mL^{-1}$) were dissolved in 10 mM sodium acetate at pH 4.5 and immobilized on separate chips at a flow rate of 30 $\mu L \cdot min^{-1}$ in NaCl/$P_i$ (Gibco, Carlsbad, CA, USA). Each chip contained a second flow cell, which was uncoated to provide negative controls. All sensorgram data presented were subtracted from the corresponding data from the blank cell. The response generated from the injection of buffer over the chip was also subtracted from all sensorgrams. Equilibrium dissociation constants ($K_D$) were calculated using BIACORE X100 evaluation software version 1.0.

For inhibition assays, 1 μM samples of $rFnBPB_{163–480}$ [10] were preincubated with doubling dilutions of $MgCl_2$, $NiCl_2$ or $CaCl_2$ for 1 h at room temperature. These solutions were then passed over the surface of rGST γ-chain-coated chips. The level of binding (RU) at equilibrium was calculated as a percentage of the RU reached by a cation-free control, and plotted against the cation concentration.

### Binding of $rFnBPB_{163–480}$ to immobilized Fn fragments

A number of functional Fn fragments were generated by the steady digestion of human Fn with thermolysin. These fragments included a 29 kDa fragment containing the five N-terminal F1 modules (N29), a 45-kDa fragment consisting of four F1 modules and two F2 modules (GBD), C-terminal fragments 607–1265 and 1266–1908, each consisting of multiple F3 modules, and C-terminal fragment 1913–2477 containing one F3 module and three F1 modules (Fig. 8A). Equal amounts of Fn and Fn fragments were dotted onto a nitrocellulose membrane and probed with $rFnBPB_{163–480}$. Bound recombinant protein was detected using rabbit polyclonal anti-$rFnBPB_{163–480}$ serum, followed by horseradish peroxidase-conjugated goat anti-rabbit IgG antibodies.

### Bacterial adhesion to immobilized El

Bacterial adhesion to immobilized El peptides was performed as described previously [6]. Briefly, microtitre plate wells (Porvair Sciences, Leatherhead, UK) were coated with various concentrations of human aortic El (Elastin Products Co, Owensville, MI, USA) and then air dried under UV light (366 nm) at room temperature for 18 h. Wells were blocked for 2 h at 37 °C with 5% (w/v) bovine serum albumin. *Staphylococcus epidermidis* cultures were grown to exponential phase, washed in NaCl/$P_i$ and resuspended to an absorbance at 600 nm of 2.0. Bacterial cell adherence was measured using a fluorescent nucleic acid stain SYTO-13 (Molecular Probes, Carslbad, CA, USA). Bacterial cells were incubated with SYTO-13 (2.5 μM) at room temperature for 15 min in the dark. El-coated wells were washed three times with NaCl/$P_i$. One hundred microlitres of stained cells were added to the plate and incubated in the dark for 90 min. Wells were washed three times with NaCl/$P_i$ and adherent bacteria were measured using an LS-50B spectrophotometer (Perkin-Elmer, Waltham, MA, USA) with excitation at 488 nm and emission at 509 nm.

### Bacterial adhesion to immobilized Fg and Fn

Bacterial adhesion to immobilized Fg and Fn was performed as described previously [23]. Briefly, microtitre plate wells were coated with various concentrations of human Fg or Fn and incubated at 4 °C for 18 h. Wells were blocked and incubated with bacteria as indicated above. Adherent cells were fixed with formaldehyde (25% v/v) for 15 min and then stained with crystal violet (0.5% w/v) for 1 min. The wells were washed extensively with NaCl/$P_i$ to remove excess stain. Cell-bound crystal violet was solubilized using acetic acid (5% v/v) and the absorbance at 570 nm was measured using an ELISA plate reader (Multiskan EX, Labsystems, Fisher Scientific, Dublin, Ireland).

## Acknowledgements

T.J.F. would like to thank Science Foundation Ireland (Programme Investigator Grant 08/IN). P.S. acknowledges Fondazione CARIPLO for a grant 'Vaccines 2009-3546'.

## References

1 Williams RE (1963) Healthy carriage of *Staphylococcus aureus*: its prevalence and importance. *Bacteriol Rev* **27**, 56–71.

2 Fowler VG Jr, Miro JM, Hoen B, Cabell CH, Abrutyn E, Rubinstein E, Corey GR, Spelman D, Bradley SF, Barsic B *et al.* (2005) *Staphylococcus aureus* endocarditis: a consequence of medical progress. *J Am Med Assoc* **293**, 3012–3021.

3 Fowler T, Wann ER, Joh D, Johansson S, Foster TJ & Hook M (2000) Cellular invasion by *Staphylococcus aureus* involves a fibronectin bridge between the bacterial fibronectin-binding MSCRAMMs and host cell beta1 integrins. *Eur J Cell Biol* **79**, 672–679.
4 Sinha B, Francois PP, Nusse O, Foti M, Hartford OM, Vaudaux P, Foster TJ, Lew DP, Herrmann M & Krause KH (1999) Fibronectin-binding protein acts as *Staphylococcus aureus* invasin via fibronectin bridging to integrin alpha5beta1. *Cell Microbiol* **1**, 101–117.
5 Jonsson K, Signas C, Muller HP & Lindberg M (1991) Two different genes encode fibronectin binding proteins in *Staphylococcus aureus*. The complete nucleotide sequence and characterization of the second gene. *Eur J Biochem* **202**, 1041–1048.
6 Roche FM, Downer R, Keane F, Speziale P, Park PW & Foster TJ (2004) The N-terminal A domain of fibronectin-binding proteins A and B promotes adhesion of *Staphylococcus aureus* to elastin. *J Biol Chem* **279**, 38433–38440.
7 Wann ER, Gurusiddappa S & Hook M (2000) The fibronectin-binding MSCRAMM FnbpA of *Staphylococcus aureus* is a bifunctional protein that also binds to fibrinogen. *J Biol Chem* **275**, 13863–13871.
8 Signas C, Raucci G, Jonsson K, Lindgren PE, Anantharamaiah GM, Hook M & Lindberg M (1989) Nucleotide sequence of the gene for a fibronectin-binding protein from *Staphylococcus aureus*: use of this peptide sequence in the synthesis of biologically active peptides. *Proc Natl Acad Sci USA* **86**, 699–703.
9 McDevitt D, Francois P, Vaudaux P & Foster TJ (1995) Identification of the ligand-binding domain of the surface-located fibrinogen receptor (clumping factor) of *Staphylococcus aureus*. *Mol Microbiol* **16**, 895–907.
10 Burke FM, McCormack N, Rindi S, Speziale P & Foster TJ (2010) Fibronectin-binding protein B variation in *Staphylococcus aureus*. *BMC Microbiol* **10**, 160.
11 Loughman A, Fitzgerald JR, Brennan MP, Higgins J, Downer R, Cox D & Foster TJ (2005) Roles for fibrinogen, immunoglobulin and complement in platelet activation promoted by *Staphylococcus aureus* clumping factor A. *Mol Microbiol* **57**, 804–818.
12 O'Connell DP, Nanavaty T, McDevitt D, Gurusiddappa S, Hook M & Foster TJ (1998) The fibrinogen-binding MSCRAMM (clumping factor) of *Staphylococcus aureus* has a $Ca^{2+}$-dependent inhibitory site. *J Biol Chem* **273**, 6821–6829.
13 Deivanayagam CC, Wann ER, Chen W, Carson M, Rajashankar KR, Hook M & Narayana SV (2002) A novel variant of the immunoglobulin fold in surface adhesins of *Staphylococcus aureus*: crystal structure of the fibrinogen-binding MSCRAMM, clumping factor A. *EMBO J* **21**, 6660–6672.
14 Ganesh VK, Rivera JJ, Smeds E, Ko YP, Bowden MG, Wann ER, Gurusiddappa S, Fitzgerald JR & Hook M (2008) A structural model of the *Staphylococcus aureus* ClfA–fibrinogen interaction opens new avenues for the design of anti-staphylococcal therapeutics. *PLoS Pathog* **4**, e1000226.
15 Keane FM, Loughman A, Valtulina V, Brennan M, Speziale P & Foster TJ (2007) Fibrinogen and elastin bind to the same region within the A domain of fibronectin binding protein A, an MSCRAMM of *Staphylococcus aureus*. *Mol Microbiol* **63**, 711–723.
16 Schwarz-Linek U, Werner JM, Pickford AR, Gurusiddappa S, Kim JH, Pilka ES, Briggs JA, Gough TS, Hook M, Campbell ID *et al.* (2003) Pathogenic bacteria attach to human fibronectin through a tandem beta-zipper. *Nature* **423**, 177–181.
17 Meenan NA, Visai L, Valtulina V, Schwarz-Linek U, Norris NC, Gurusiddappa S, Hook M, Speziale P & Potts JR (2007) The tandem beta-zipper model defines high affinity fibronectin-binding repeats within *Staphylococcus aureus* FnBPA. *J Biol Chem* **282**, 25893–25902.
18 Que YA, Francois P, Haefliger JA, Entenza JM, Vaudaux P & Moreillon P (2001) Reassessing the role of *Staphylococcus aureus* clumping factor and fibronectin-binding protein by expression in *Lactococcus lactis*. *Infect Immun* **69**, 6296–6302.
19 Que YA, Haefliger JA, Piroth L, Francois P, Widmer E, Entenza JM, Sinha B, Herrmann M, Francioli P, Vaudaux P *et al.* (2005) Fibrinogen and fibronectin binding cooperate for valve infection and invasion in *Staphylococcus aureus* experimental endocarditis. *J Exp Med* **201**, 1627–1635.
20 Kuusela P, Vartio T, Vuento M & Myhre EB (1984) Binding sites for streptococci and staphylococci in fibronectin. *Infect Immun* **45**, 433–436.
21 Bozzini S, Visai L, Pignatti P, Petersen TE & Speziale P (1992) Multiple binding sites in fibronectin and the staphylococcal fibronectin receptor. *Eur J Biochem* **207**, 327–333.
22 Sakata N, Jakab E & Wadstrom T (1994) Human plasma fibronectin possesses second binding site(s) to *Staphylococcus aureus* on its C-terminal region. *J Biochem* **115**, 843–848.
23 Hartford O, Francois P, Vaudaux P & Foster TJ (1997) The dipeptide repeat region of the fibrinogen-binding protein (clumping factor) is required for functional expression of the fibrinogen-binding domain on the *Staphylococcus aureus* cell surface. *Mol Microbiol* **25**, 1065–1076.
24 Fitzgerald JR, Loughman A, Keane F, Brennan M, Knobel M, Higgins J, Visai L, Speziale P, Cox D & Foster TJ (2006) Fibronectin-binding proteins of *Staphylococcus aureus* mediate activation of human platelets via fibrinogen and fibronectin bridges to integrin GPIIb/IIIa and IgG binding to the FcgammaRIIa receptor. *Mol Microbiol* **59**, 212–230.

25 Palmqvist N, Silverman GJ, Josefsson E & Tarkowski A (2005) Bacterial cell wall-expressed protein A triggers supraclonal B-cell responses upon in vivo infection with *Staphylococcus aureus*. *Microbes Infect* **7**, 1501–1511.
26 Ponnuraj K, Bowden MG, Davis S, Gurusiddappa S, Moore D, Choe D, Xu Y, Hook M & Narayana SV (2003) A 'dock, lock, and latch' structural model for a staphylococcal adhesin binding to fibrinogen. *Cell* **115**, 217–228.
27 Edwards AM, Potts JR, Josefsson E & Massey RC (2010) *Staphylococcus aureus* host cell invasion and virulence in sepsis is facilitated by the multiple repeats within FnBPA. *PLoS Pathog* **6**, e1000964.
28 Sambrook J, Fritsch EF & Maniatis T (1989) *Molecular Cloning: A Laboratory Manual*, 2nd edn. Cold Spring Harbor Laboratory Press, Cold Spring Harbor, New York.
29 Augustin J & Gotz F (1990) Transformation of *Staphylococcus epidermidis* and other staphylococcal species with plasmid DNA by electroporation. *FEMS Microbiol Lett* **54**, 203–207.
30 Augustin J, Rosenstein R, Wieland B, Schneider U, Schnell N, Engelke G, Entian KD & Gotz F (1992) Genetic analysis of epidermin biosynthetic genes and epidermin-negative mutants of *Staphylococcus epidermidis*. *Eur J Biochem* **204**, 1149–1154.